JGR Oceans

RESEARCH ARTICLE
10.1029/2019JC014940

Special Section:
Forum for Arctic Modeling and Observational Synthesis (FAMOS) 2: Beaufort Gyre Phenomenon

Deepening of the Winter Mixed Layer in the Canada Basin, Arctic Ocean Over 2006–2017

Sylvia T. Cole[1] and **James Stadler**[2]

[1]Woods Hole Oceanographic Institution, Woods Hole, MA, USA, [2]Haverford College, Haverford, PA, USA

Key Points:
- The winter mixed layer in the Canada Basin was 9-m deeper on average over 2013–2017 compared with 2006–2012
- Mixed layer density increased by 0.5 kg/m^3 and stratification at the mixed layer base decreased
- Mixed layer deepening was inferred to result from changes in freshwater accumulation and/or storage that increased mixed layer salinity

Correspondence to:
S. T. Cole,
scole@whoi.edu

Citation:
Cole, S. T., & Stadler, J. (2019). Deepening of the winter mixed layer in the Canada Basin, Arctic Ocean over 2006–2017. *Journal of Geophysical Research: Oceans*, *124*, 4618–4630. https://doi.org/10.1029/2019JC014940

Received 3 JAN 2019
Accepted 15 JUN 2019
Accepted article online 22 JUN 2019
Published online 8 JUL 2019

Abstract The Arctic Ocean mixed layer interacts with the ice cover above and warmer, nutrient-rich waters below. Ice-Tethered Profiler observations in the Canada Basin of the Arctic Ocean over 2006–2017 are used to investigate changes in mixed layer properties. In contrast to decades of shoaling since at least the 1980s, the mixed layer deepened by 9 m from 2006–2012 to 2013–2017. Deepening resulted from an increase in mixed layer salinity that also weakened stratification at the base of the mixed layer. Vertical mixing alone can explain less than half of the observed change in mixed layer salinity, and so the observed increase in salinity is inferred to result from changes in freshwater accumulation via changes to ice-ocean circulation or ice melt/growth and river runoff. Even though salinity increased, the shallowest density surfaces deepened by 5 m on average suggesting that Ekman pumping over this time period remained downward. A deeper mixed layer with weaker stratification has implications for the accessibility of heat and nutrients stored in the upper halocline. The extent to which the mixed layer will continue to deepen appears to depend primarily on the complex set of processes influencing freshwater accumulation.

Plain Language Summary The upper tens of meters of the Arctic Ocean, termed the mixed layer, separate the floating sea ice above from warmer and nutrient-rich waters below. Observations in winter are used to investigate changes to the mixed layer over 2006–2017. The mixed layer has recently gotten thicker (deeper) by 9 m, in contrast to past decades where it thinned (shoaled). Deepening resulted from changes to ocean salinity in the mixed layer that cannot be explained by mixing with saltier water below. Thus, the increase in mixed layer salinity is inferred to result from interannual changes to the ice-ocean circulation, ice melt/growth, or river runoff. Changes to water properties also occurred in the region immediately beneath the mixed layer, making it energetically easier for heat to be combined into the mixed layer. The extent to which the mixed layer will continue to deepen appears to depend primarily on the complex set of processes that can influence mixed layer salinity.

1. Introduction

The Arctic Ocean mixed layer is coupled dynamically and thermodynamically with the ice cover above (e.g., McPhee, 2012), while the strong stratification at the mixed layer base effectively isolates heat and nutrients from the upper tens of meters of the water column (Maykut & McPhee, 1995; Shaw et al., 2009). The mixed layer in the Canada Basin is shallow, less than 50-m deep in winter and shoaling to 20 m or less in summer (Peralta-Ferriz & Woodgate, 2015; Toole et al., 2010). The shallow winter mixed layer results from limited vertical mixing together with buoyant freshwater input (as salinity has the largest influence on density at cold Arctic temperatures). Freshwater accumulates in the Canada Basin due to the Beaufort Gyre, an anticyclonic circulation of the ice and upper ocean driven by surface winds that retains fresh surface waters via Ekman convergences. Interannual changes to the mixed layer are influenced by processes that affect vertical mixing or surface freshwater including ice melt/growth, river runoff, surface circulation, areas of open water (changes to ice extent or leads) where the wind can directly force the ocean (Krishfield et al., 2014; McPhee, 2013; Proshutinsky et al., 2009; Zhang et al., 2016), and internal wave breaking near the mixed layer base (e.g., D'Asaro & Morison, 1992). Mixed layer feedbacks with the ice cover make future changes to the Arctic ice cover and upper ocean stratification difficult to predict. There is a wide range of potential outcomes for the ice cover itself (Carmack et al., 2015), and the nutrients and ecosystems residing within and beneath the mixed layer, which are all sensitive to changes in mixed layer depth and/or entrainment.

Observations over 1980–2008 have indicated that the Canada Basin winter mixed layer has shoaled due to increased freshwater accumulation. Based on November–May observations that are interannually sparse,

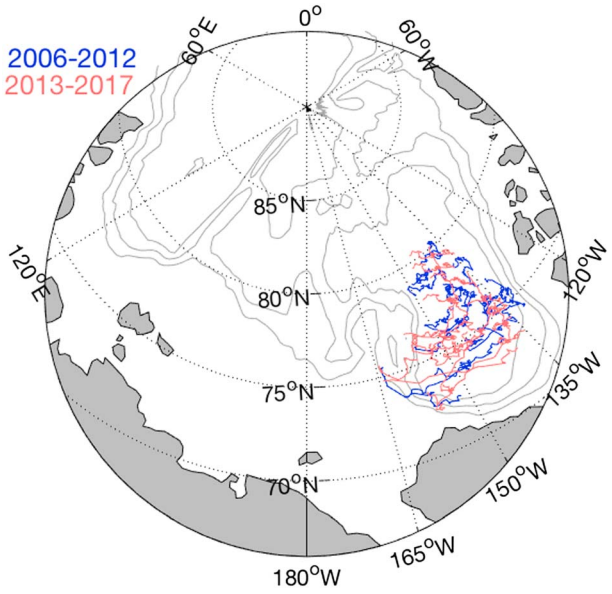

Figure 1. Map of each January–May ITP record during 2006–2012 (blue) and 2013–2017 (red).

the winter mixed layer trend reported for the period 1980–2008 is a shoaling of 0.64 m/year, amounting to 19 m over 30 years (Peralta-Ferriz & Woodgate, 2015). Similarly, the trend in winter mixed layer salinity was a freshening of 0.19 psu/year or 5.5 psu over 1980–2008 (Peralta-Ferriz & Woodgate, 2015). Freshening extends throughout the upper few hundred meters of the water column and has occurred due to increased ice melt and river runoff as well as Ekman convergence of surface waters that resulted from increased anticyclonic wind stress (Krishfield et al., 2014; Proshutinsky et al., 2009; Zhang et al., 2016). Mixed layer shoaling due to freshwater accumulation (and weak vertical mixing) occurred simultaneously with increased Ekman pumping that has deepened the average depth of density surfaces in the upper halocline (Timmermans et al., 2014; Zhang et al., 2016). Interannual changes to freshwater content (and inferred changes to freshwater accumulation) are better observed than changes to vertical mixing within or at the base of the mixed layer. It is inconclusive to what extent vertical mixing at any depth may be changing interannually (e.g., Guthrie et al., 2013). Whether or at what rate the future mixed layer will continue to shoal is an open question.

Several recent studies have focused on changes to the ice cover and ocean circulation over the last decade but do not address in detail how the mixed layer has been affected. Sea ice extent and thickness have continued to decline, with a historic minimum in extent in summer 2012 (Carmack et al., 2015; Comiso, 2012; Kwok et al., 2009). Sea ice velocity is increasing along with wind speeds (Carmack et al., 2015; Kwok et al., 2013). The Beaufort Gyre ice and ocean circulation intensified over 1995–2008 and then stabilized over 2008–2015 (Armitage et al., 2017; Krishfield et al., 2014; McPhee, 2013; Zhang et al., 2016). Increased Ekman convergence during the spin-up period led to freshwater accumulation within the upper 400 m (Krishfield et al., 2014; Proshutinsky et al., 2009), while the stabilization period has been associated with increased mixed layer salinity (Zhang et al., 2016). These recent dynamic changes, that is, the stabilization of the Beaufort Gyre together with decreased sea ice extent in summer, have the potential to influence the Canada Basin mixed layer.

This paper focuses on the winter mixed layer, which is historically underobserved due to limited ship access in winter months. We are interested in the interannual and large-scale changes to the mixed layer, not the variations in mixing layers that are indicative of mixing over a number of days (see section 3). Ice-Tethered Profiler observations since 2006 reveal that the decade-long shoaling trend of the winter mixed layer in the Canada Basin has reversed.

2. Data

2.1. Ice-Tethered Profilers

We utilize temperature and salinity profiles in the Canada Basin of the Arctic Ocean from Ice-Tethered Profilers (ITPs; Toole et al., 2011; downloaded in March 2019 from www.whoi.edu/itp). The region south of 80.5°N and west of 165°W in the Canada Basin is considered, limiting the analysis to the Beaufort Gyre region (see Regan et al., 2019). To focus on the winter mixed layer, January through May data for each ITP and year are treated as separate records. These months are selected to avoid months when the mixed layer may be seasonally deepening or shoaling. Only records longer than 30 days are used. A total of 36 winter records are available over 2006–2017 that meet these criteria (Figure 1), with further details of these records provided in Table 1.

Eight records do not yet have fully processed temperature and salinity data available; we use the level II data product for these records (Krishfield et al., 2008). Downward profiles are excluded from analysis of level II data, as these have known biases due to the profiler wake that are not corrected in this level of processing. The vertical resolution of the level II products is 2 dbar compared with 1 dbar for all other ITP data. A total of 12,148 profiles are included in the analysis, of which 1,065 are level II data. A direct comparison of level II

Table 1
Details of the January–May ITP Records Used in This Analysis

Record number[a]	ITP number	Year	Dates	Processing	Number of profiles[b]
1	ITP-1	2006	1/1–5/31	Final	602
2	ITP-3	2006	1/1–5/31	Final	597
3	ITP-5	2007	1/1–5/31	Final	393
4	ITP-6	2007	1/1–5/31	Final	297
5	ITP-4	2007	1/1–5/31	Final	300
6	ITP-8	2008	1/1–5/31	Final	301
7	ITP-13	2008	1/1–5/31	Final	314
8	ITP-18	2008	1/1–5/31	Final	274
9	ITP-8	2009	1/1–5/31	Final	148
10	ITP-11	2009	1/1–5/31	Final	314
11	ITP-33	2010	1/1–5/31	Final	275
12	ITP-34	2010	1/1–3/30	Final	175
13	ITP-32	2010	1/1–2/9	Final	76
14	ITP-35	2010	1/1–3/31	Final	514
15	ITP-43	2011	1/1–2/11	Final	41
16	ITP-41	2011	1/1–5/31	Final	296
17	ITP-42	2011	1/1–4/15	Final	200
18	ITP-53	2012	1/1–5/31	Final	278
19	ITP-41	2012	1/1–5/31	Final	301
20	ITP-62	2013	1/1–5/31	Final	275
21	ITP-65	2013	1/1–5/31	Final	426
22	ITP-64	2013	1/1–5/31	Final	418
23	ITP-70	2014	1/1–5/31	Final	1203
24	ITP-69	2014	1/1–2/15	Final	46
25	ITP-77	2014	3/10–5/31	Final	657
26	ITP-78	2014	3/11–5/31	Final	649
27	ITP-79	2014	3/21–5/31	Final	569
28	ITP-80	2015	1/1–5/24	Final	1144
29	ITP-85	2015	1/1–5/31	Level II	151
30	ITP-81	2015	1/1–5/31	Level II	151
31	ITP-86	2015	1/1–5/31	Level II	149
32	ITP-87	2015	1/1–5/31	Level II	148
33	ITP-82	2015	1/1–5/31	Level II	151
34	ITP-82	2016	1/1–3/10	Level II	47
35	ITP-89	2016	1/1–5/31	Level II	121
36	ITP-97	2017	1/1–5/31	Level II	147

Note. Date format is month/day.
[a]Records are arranged in the order in which they are plotted in Figures 3a and 3b. [b]Number of profiles with a mixed layer depth estimate.

upward profiles and the final (level III) data processing shows that differences in mixed layer depth or salinity are minor (e.g., less than 1 m on average for mixed layer depth; not shown).

The ITP systems record at least two (one upward, one downward) profiles of temperature and salinity each day. Some systems were programmed to sample more frequently in time, up to 8 profiles per day, and so there are between 30 profiles (a single month of level II data) and 1,200 profiles (5 months of highly sampled data) within each of the 36 January–May records (Table 1).

To evaluate potential changes to mechanical mixing within the mixed layer (as opposed to thermodynamically driven mixing), the ice velocity during each record is considered. Ice velocity is estimated from hourly GPS positions of the ITP surface unit. Ice velocity is then interpolated to the corresponding times of each profile, and the speed is then estimated.

2.2. Ice Concentration

Special Sensor Microwave/Imager (SSM/I) ice concentration (Cavalieri et al., 1996) is utilized as it spans the entire record and is sufficient to show the interannual changes in January–May ice cover. Ice concentration was interpolated to the times and locations of the ITP profiles used in this analysis.

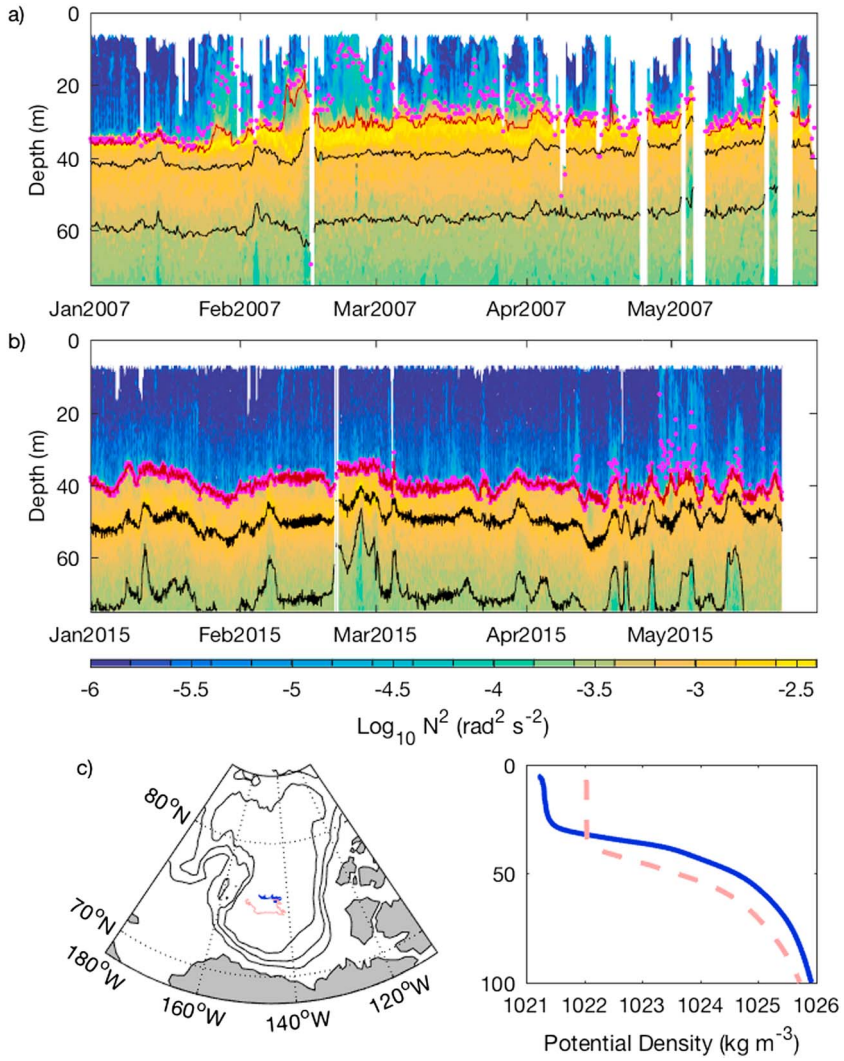

Figure 2. Example time series of buoyancy frequency for (a) ITP-5 in 2007 and (b) ITP-80 in 2015. The mixed layer base (dark red line) and mixing layer base (magenta dots) are estimated using 0.25 and 0.03 kg/m^3 potential density thresholds, respectively, and sometimes coincide. The 1,023.5 and 1,025.0 kg/m^3 potential density surfaces (black) are also shown. Note that ITP-5 profiled twice per day, while ITP-80 profiled eight times per day causing the black and dark red lines to appear thicker for ITP-80 as internal wave variability is resolved in more detail. (c) Map of profile locations and (d) average potential density for ITP-5 (blue) and ITP-80 (red).

3. Methods

There is not a universal definition of mixed layer depth in the Arctic Ocean, and density thresholds of 0.01 to 0.25 kg/m^3 appear in the literature (Peralta-Ferriz & Woodgate, 2015; Timmermans et al., 2012; Toole et al., 2010). Here, three different potential density thresholds from the shallowest observation are considered: 0.03, 0.10, and 0.25 kg/m^3. The mixed layer depth refers to the 0.25 kg/m^3 density threshold and is the focus of this study as it is indicative of the large-scale structure of the Beaufort Gyre. With this definition, mixed layer depth represents the depth to which water has mixed over the winter season and accurately tracks the region of elevated stratification and shear (Figures 2a and 2b). An alternate definition of mixed layer depth using a 0.10 kg/m^3 density threshold was also considered, and all results are found to be robust to the choice of density threshold (see section 5). In addition to these definitions of a mixed layer, we consider a mixing layer base defined using a density threshold of 0.03 kg/m^3 for illustrative purposes. Mixing layer depth is representative of weak stratification within the mixed layer often associated with submesoscale fronts (Timmermans et al., 2012). We do not consider statistics of the mixing layer here. Note that due to

the occasional presence of shallow mixing layers (e.g., Figures 2a and 2b), we consider statistics of the potential density at the base of the mixed layer (e.g., a mean value of 1,021.6 kg/m^3 for ITP-5; Figure 2a), which is greater than the average potential density within the mixed layer (e.g., a mean value of 1,021.4 kg/m^3 for ITP-5; Figure 2a).

The shallowest observation was typically at ~7-m depth, although it was sporadically deeper for some profiles (e.g., Figure 2). Missing observations in the upper few meters were not crucial for determining the mixed layer depth in winter (whereas in summer, they can be). Only six profiles were excluded from analysis due to insufficient data in the upper tens of meters.

To evaluate interannual changes taking place in waters just beneath the mixed layer, the depth of the 1023.5 kg/m^3 potential density surface is considered. It is the shallowest potential density surface present throughout all records and often resides less than 10 m beneath the mixed layer base (e.g., Figure 2). Changes to the mean depth of the 1,023.5 kg/m^3 potential density surface are indicative of Ekman pumping in the uppermost portions of the halocline (see section 4.1).

To evaluate how a changing mixed layer may impact the ice cover, the ocean heat content, and the amount of ice that heat can melt, are considered. Heat content relative to the freezing temperature is estimated for each profile as $Q = \rho_0 c_p \int (T - T_f) dz$, where ρ_0 = 1,023 kg/m^3 is a reference value, C_p = 3,986 J kg^{-1} °C^{-1} is the specific heat capacity, and T_f is the freezing temperature of seawater. The reference salinity used in estimating the freezing temperature is the average salinity of the region considered, which is the 0.5 kg/m^3 potential density range immediately beneath the mixed layer base (discussed further in section 4). The amount of ice that can be melted is estimated as $\Delta z_{ice} = Q/\rho_{ice}/q_{lh}$, where ρ_{ice} = 910 kg/m^3 is the density of the ice and $q_{lh} = 3 \times 10^5$ J/kg is the latent heat of fusion for sea ice.

Liquid freshwater content is also estimated for each profile. Following Proshutinsky et al. (2009), liquid freshwater content is estimated as $\int (S_{ref} - S(z))/S_{ref} dz$ where a reference salinity of 34.8 g/kg is used (see also Aagaard & Carmack, 1989). The integral is calculated from 2-m depth to the depth at which salinity equals the reference salinity, with the shallowest salinity value extrapolated to 2-m depth (so that no portion of the upper water column is excluded). The reference salinity is at approximately 350- to 400-m depth, and so this is a relative measure of the freshwater in the upper ocean that can be used to investigate freshwater variability. The liquid freshwater content is also considered as the integral from 2 m to the 29.2 g/kg salinity surface that resides a few meters beneath the base of the mixed layer (and corresponds to the 1023.5 kg/m^3 potential density surface on average) to give an estimate of freshwater content of this uppermost region.

4. Results

4.1. Mixed Layer Conditions

Representative ITP records from the central Beaufort Gyre (74–75°N, 140–153°W) illustrate the changes to winter mixed layer properties that occurred during 2006–2017 (Figure 2). Observed winter mixed layers sampled by ITP-80 in 2015 were 9-m deeper on average (40.2 m versus 31.0 m) than those sampled by ITP-5 in 2007. Potential density surfaces in the halocline also deepened. The 1,023.5 kg/m^3 isopycnal, which was 7–8 m below the mixed layer base in both records, deepened by 11 m (39 m versus 50 m on average), suggesting downward Ekman pumping of the upper halocline between the ITP-5 observations in 2007 and the ITP-80 observations in 2015. Mean potential density profiles show that the mixed layer became denser as well as deeper (Figure 2d), suggesting that some vertical mixing or increase in salinity occurred (due to a change in the freshwater budget, e.g., decreased melting or river runoff).

The ITP data set of 36 records for the January–May period shows the interannual variability in mixed layer depth (Figure 3a). Despite variability within (e.g., Figures 2a and 2b) and between records, the data reveal a clear interannual change with the shallowest winter mixed layers observed in 2008–2009, and the deepest winter mixed layers in 2014–2017. For detailed analysis, the data were partitioned into the time periods of 2006–2012 and 2013–2017. The two groups show a significant difference in the mixed layer depth distributions (Figure 3c). Mean mixed layer depths were 9.1-m deeper over 2013–2017 (mean ± standard error of 39.3 ± 0.1 m) versus 2006–2012 (mean ± standard error of 30.2 ± 0.1 m).

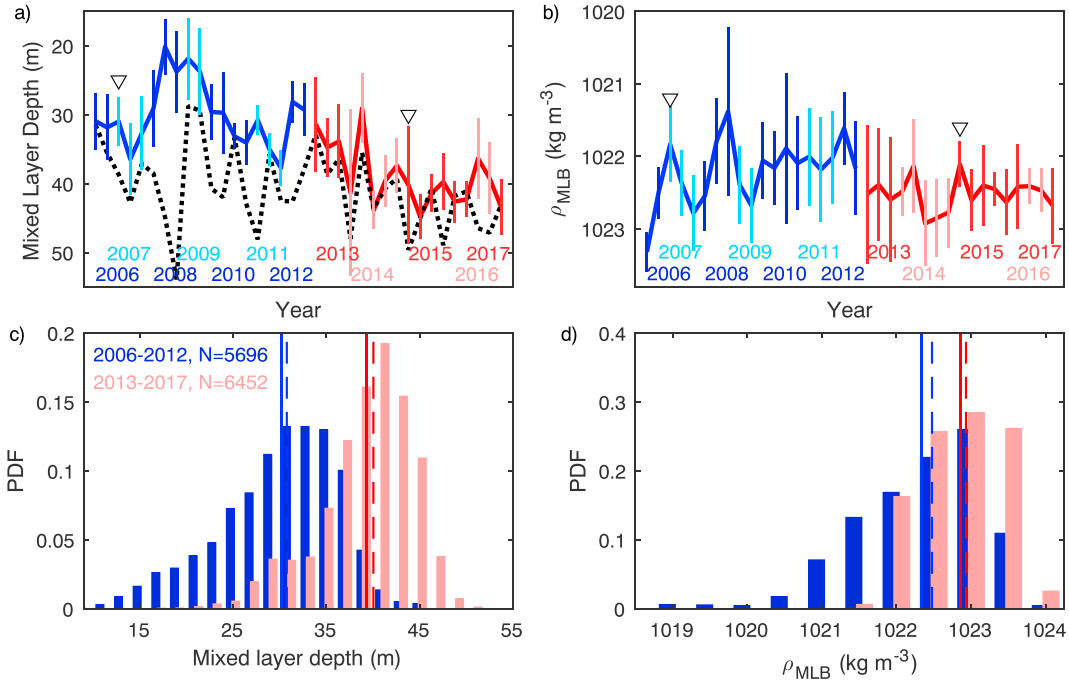

Figure 3. Mean (thick line) and standard deviation (thin vertical bars) for each January–May record of (a) mixed layer depth and (b) density at the mixed layer base, ρ_{MLB}. Blue denotes 2006–2012 and red denotes 2013–2017 with each year in light or dark shading and records plotted in the order listed in Table 1. Triangles indicate ITP-5 and ITP-80 records shown in Figure 2. The mean depth of the 1,023.5 kg/m^3 density surface (dotted black) is shown in (a). Probability density functions over 2006–2012 and 2013–2017 of (c) mixed layer depth with the total number of profiles indicated and (d) density at the mixed layer base. Mean (solid) and median (dashed) values are indicated for each time period.

Potential density surfaces in the upper halocline also deepened over 2006–2017. The 1023.5 kg/m^3 isopycnal had a mean depth of 38.8 m in 2006–2012 and 43.7 m in 2013–2017 (Figure 3a), an increase of 4.9 m (compared with an increase of 9.1 m for the mixed layer base). The interannual variability of the depth of the 1,023.5 kg/m^3 isopycnal did not perfectly follow that of the mixed layer, with the two variables exhibiting obvious covariability only during 2013–2017. Deeper in the water column, the 1,025.0 kg/m^3 isopycnal had a mean depth of 62.7 m in 2006–2012 and 64.2 m in 2006–2012, an increase of 1.5 m. For both the 1023.5 and 1025.0 kg/m^3 potential density surfaces, probability density functions (PDFs) during the two time periods were significantly different at the 99% confidence interval (not shown).

The mean density at the base of the mixed layer, ρ_{MLB}, was 0.51 kg/m^3 denser over 2013–2017 (mean ± standard error of 1,022.34 ± 0.01 kg/m^3 versus 1,022.85 ± 0.01 kg/m^3 over 2006–2012), consistent with vertical entrainment across the mixed layer base and/or a net reduction in freshwater input to the mixed layer (Figures 3b and 3d). PDFs of density at the mixed layer base were significantly different at the 99% confidence level (Figure 3d).

To address whether these density and salinity changes could have resulted from one-dimensional vertical mixing, artificial salinity and density profiles are constructed by vertically mixing the 2006–2012 mean salinity and density profiles by an additional 4 m (e.g., salinity profiles in Figure 4b). Four meters is chosen as it is the difference between the 9.1-m mixed layer deepening and 4.9 m of isopycnal deepening. The mean density profile vertically mixed in this way corresponded to a mixed layer potential density that increased by 0.08 kg/m^3, less than one quarter of the observed increase in potential density between the two time periods. Note that vertically mixing by 9 m corresponds to a mixed layer potential density that increased by 0.25 kg/m^3, only half of the observed increase. Thus, a change in net freshwater input to the mixed layer is required to explain the observed increase in density at the base of the mixed layer.

Average profiles similarly show that the waters beneath the mixed layer also changed over the study period (Figure 4). The subsurface temperature maximum of Pacific Summer Water that resides at ~40- to 100-m depth increased by up to 0.6 °C during 2013–2017 (Figure 4a, see also Timmermans et al., 2018). The

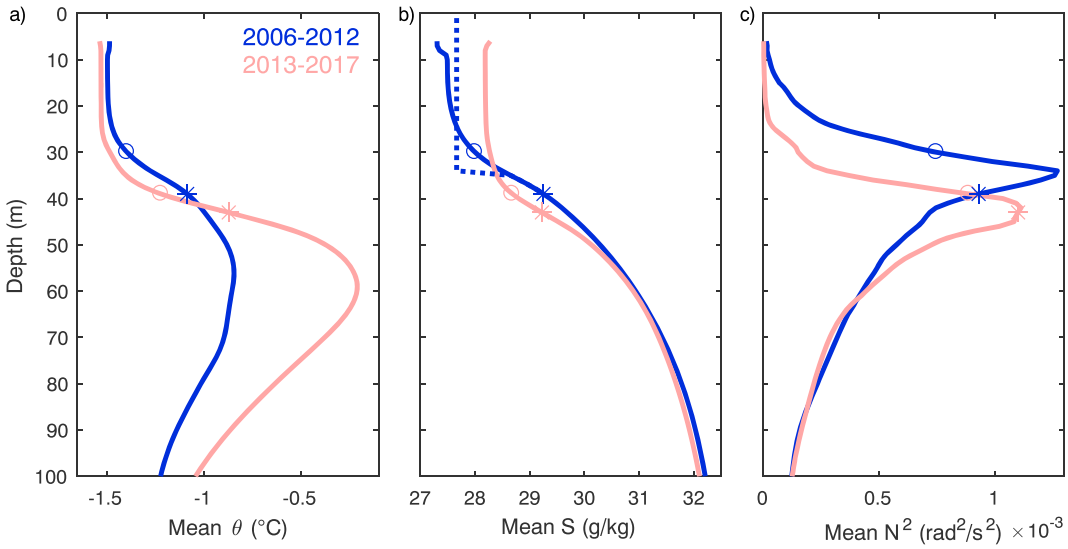

Figure 4. Average (a) potential temperature, (b) salinity, and (c) stratification profiles over 2006–2012 (blue) and 2013–2017 (red). The mean properties at the mean mixed layer depth (circles) and at 1,023.5 kg/m^3 (asterisks) are indicated for each period. Dotted blue line in (b) is the salinity profile of the 2006–2012 data after vertically mixing by an additional 4 m.

mixed layer became ~1 g/kg saltier, with nearly identical mean salinity profiles below 60 -m depth. The denser and deeper mixed layers over 2013–2017 resulted in a stratification maximum at the mixed layer base that was weaker compared to the earlier period. The upper ocean stratification in the Canada Basin (Figure 4c) was influenced by vertical mixing and/or a reduction in freshwater input to the mixed layer that increased the density of the mixed layer and the density at which the (weaker) stratification maximum occurred.

The heat content and average stratification of the region immediately beneath the mixed layer base combine to determine the extent to which one-dimensional vertical mixing can melt sea ice. Here we consider only what can be reasonably entrained, which is the 0.5 kg/m^3 density span below the mixed layer base that corresponds to the actual increase in mixed layer density over 2006–2017. This region represents the water mixed into the mixed layer for 2006–2012 profiles, and the water that could be mixed into the mixed layer for 2013–2017 profiles assuming a similar increase in mixed layer salinity were to occur in future years. The heat content relative to the freezing temperature, Q (section 3), and stratification in this region is estimated from individual profiles. In the later time period, heat content had increased (Figure 5a) and average stratification had decreased with fewer instances of both very weak and very strong stratification (Figure 5b), consistent with changes to the mean profiles (Figure 4). The average heat content in the 0.5 kg/m^3 beneath

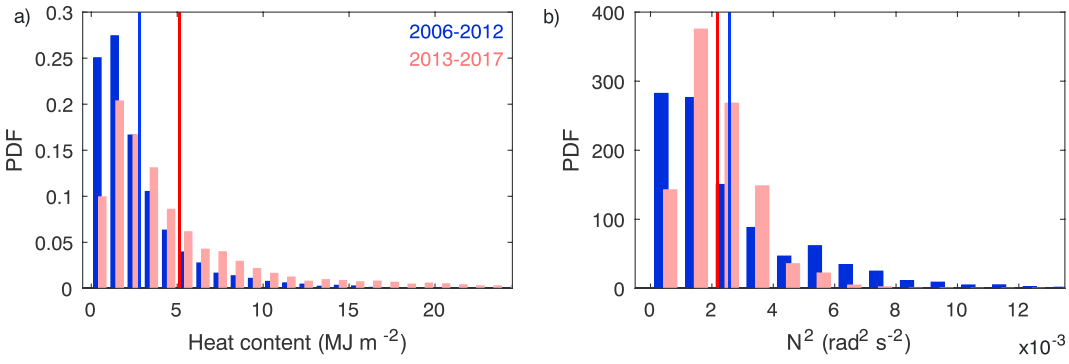

Figure 5. Probability density functions over 2006–2012 (blue) and 2013–2017 (red) of average (a) heat content and (b) stratification of the 0.5 kg/m^3 density range immediately beneath the mixed layer base. Mean (solid) and median (dashed) values are indicated for each time period.

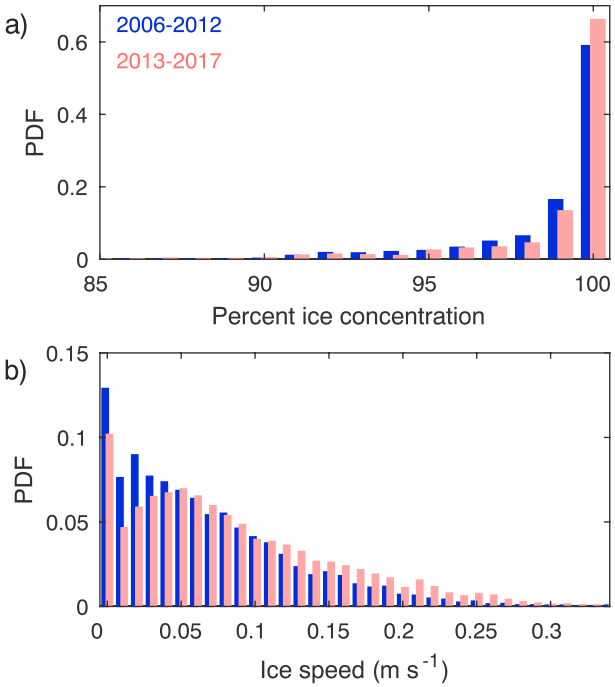

Figure 6. Ice conditions during 2006–2012 (blue) and 2013–2017 (red) showing probability density functions of (a) ice concentration and (b) ice speed.

the mixed layer base was 2.8 MJ/m^2 over 2006–2012 versus 5.1 MJ/m^2 over 2013–2017 and is enough heat to melt 0.01 m (2006–2012) and 0.02 m (2013–2017) of ice. Compared to the 0.6 m of net ice thinning that has occurred each decade (Carmack et al., 2015), vertically mixing this heat into the mixed layer accounts for less than 3% of the total melt during 2006–2012 (0.01 m) or during 2013–2017 (0.02 m assuming a continued increase in mixed layer density). The average stratification beneath the mixed layer base decreased by 16% between the time periods, making it energetically easier to vertically mix heat from the Pacific Summer Water layer.

4.2. Ice Conditions

To address whether the interannual deepening of the mixed layer depth resulted from interannual changes to the ice cover (e.g., the presence of leads) that can influence vertical mixing, ice concentration and ice speed are considered specifically for this spatial and temporal subset of the region. Values were interpolated to the profile times and locations in Figure 1. The interannual changes to ice concentration and speed are similar to those observed from instruments with more complete coverage of the Canada Basin (section 1). Ice concentrations during January–May were above 90% in both time periods with a slightly higher probability of full ice cover (100% ice concentration) over 2013–2017 (Figure 6a). Ice speed increased during 2006–2017, with a smaller proportion of ice speeds less than 0.05 m/s and median speeds of 0.07 m/s during 2013–2017 compared with 0.06 m/s during 2006–2012 (Figure 6b). Changes between the time periods were significant at the 99% confidence level for ice speed and winter ice concentration.

At deployment, the initial ice thickness of the sea ice floe on which an ITP was deployed was also recorded (a thickness of 0 m was specified for systems deployed in open water). Ice thickness was measured in a variety of ways, but the uncertainty is small compared to the bias from preferentially deploying ITPs on the most robust ice available, and in summer (33 of the records were deployed in the August–October period). The initial ice thickness estimates decreased from a mean ± standard error of 3.2 ± 0.1 m over 2006–2012 to 1.6 ± 0.2 m over 2013–2017 (not shown).

5. Discussion

5.1. Robustness of Results

While the geographic coverage of the ITP records is not uniform, there is little evidence that geographic variability influenced these results. Over the two time periods, observations are spread throughout the Beaufort Gyre, with similar changes observed in both individual records and the collective mean (Figures 2–4). Gridded maps of mixed layer depth and salinity show that these changes were large in scale, spanning the entire basin (Figure 7).

These results are also robust to alterations in the methods used to analyze the ITP data, specifically the definition of the mixed layer base and the definition of winter. Considering a mixed layer base defined using a 0.10 kg/m^3 density threshold, as was used in Peralta-Ferriz and Woodgate (2015), mixed layer depths in both time periods were slightly shallower on average (Figure 8a), with only minor differences in the density at the mixed layer base (Figure 8b). The mixed layer deepened by 10.7 m between the two time periods, a slightly larger change than when using a density threshold of 0.25 kg/m^3 (9.1 m of deepening). Considering a stricter definition of winter to be only the months of January, February, and March, the probably density functions of mixed layer depth remained largely unchanged with no significant changes to the mean mixed layer depth (Figure 8c). The increase in density at the mixed layer base between the two time periods was 0.46 kg/m^3 for the January–March subset of data, similar to the 0.51 kg/m^3 increase for the full January–May data set (Figure 8d).

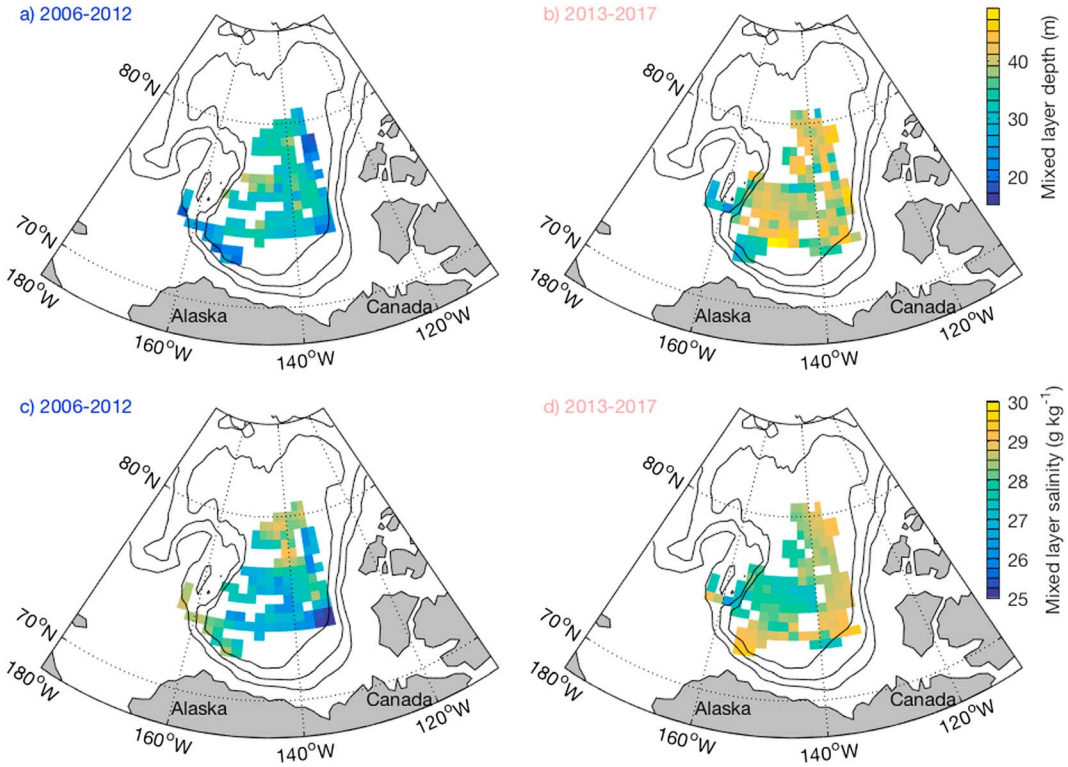

Figure 7. Gridded averages of (a and b) mixed layer depth and (c and d) salinity at 10-m depth over (a, c) 2006–2012 and (b, d) 2013–2017. Spatial gridding was done by averaging all data into bins of 2° in longitude and 0.5° in latitude (or approximately 56 × 58 km bins at these latitudes).

Alternate error estimates of mean mixed layer depth can be considered. We have given the standard error of the mean mixed layer depth in each time period assuming each profile is an independent measurement, which leads to a standard error of ±0.1 m. Assuming that measurements are independent on a weekly basis results in $N = 353$ and 307 degrees of freedom for 2006–2012 and 2013–2017, respectively, and a standard error of ±0.3 m for both time periods. As the measurements have a 1- to 2-m vertical resolution, ±1 m in 2006–2012 and ±2 m in 2013–2017 is an alternate error estimate. Even with this larger error estimate, the 9 m deepening of the mixed layer remains significant.

5.2. Causes of a Deeper, Saltier, and Denser Winter Mixed Layer

It is clear that some mechanisms are not solely responsible for the increase in mixed layer salinity. All processes associated with one-dimensional vertical mixing cannot explain the observed changes to the mixed layer, including increased mechanical mixing, or reduced stratification at the stratification maximum that could increase entrainment.

In further support of this conclusion, the indirect indicators of vertical mixing analyzed here, specifically ice speed and ice concentration (that is indicative of leads at this time of year), suggest that any changes to vertical mixing were not substantial. The observed increase in ice speeds was weak, and moreover, ice speeds increased during the decadal spin-up of the Beaufort Gyre, while the mixed layer shoaled (Kwok et al., 2013; Peralta-Ferriz & Woodgate, 2015). As there was a slight decrease between the two time periods in the fraction of open water during January–May, direct atmospheric forcing through leads (during these months) does not explain the recent increase in mixed layer depth either. It is possible that the 2012 summer ice extent minima introduced additional wind-forced mixing to the upper ocean, which then made it easier to deepen the mixed layer base during the subsequent winter. This argument is weakened as a similar ice extent minimum was observed in 2007 without a corresponding increase in mixed layer depth in the following years. While a cumulative effect of decreased ice extent influencing the mixed layer remains a possibility, ice extent can certainly have an indirect influence via modulation of processes such as Ekman pumping and

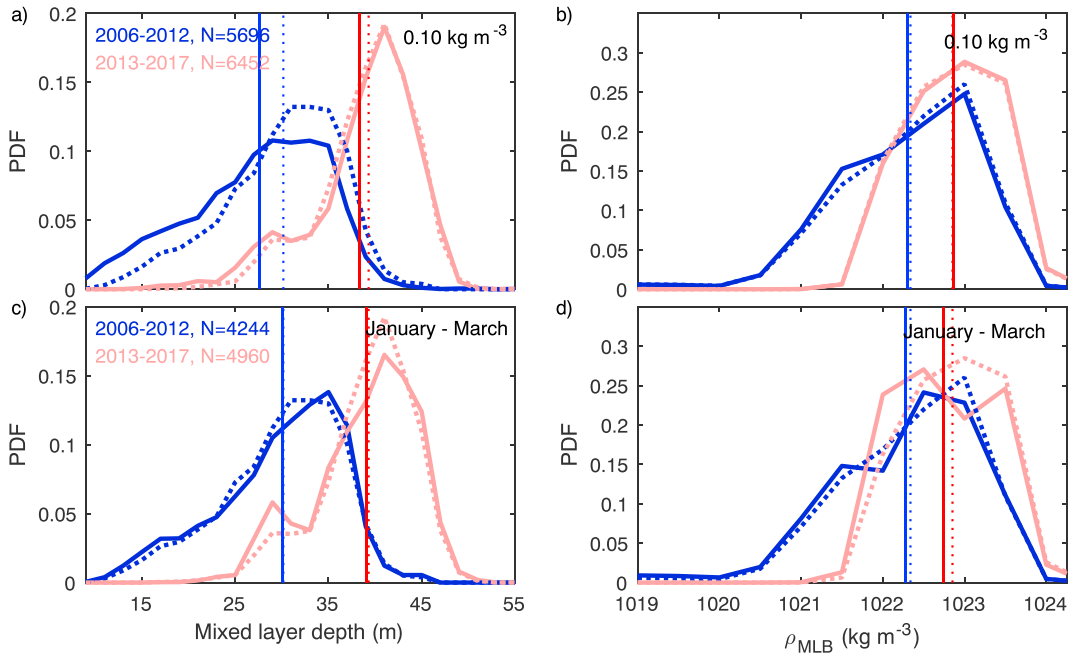

Figure 8. Probability density functions (PDFs) over 2006–2012 and 2013–2017 of (a, c) mixed layer depth with the total number of profiles indicated and (b, d) density at the mixed layer base. In (a) and (b), a mixed layer defined using the 0.25 kg/m^3 density threshold (dotted; as in Figures 3c and 3d) is compared to a 0.10 kg/m^3 density threshold (solid). In Figures 3c and 3d), the full January–May data set (dotted; as in Figures 3c and 3d) is compared with a subset of the data that includes only January–March profiles (solid). Mean values are indicated for each time period (solid and dotted).

Ekman convergence of surface waters. Overall, it is not possible, from our ITP data, to conclude whether the strength of vertical mixing at the mixed layer base changed over 2006–2017.

Beyond the conclusion that vertical mixing is not the sole cause of increased mixed layer salinity, the exact mechanism can only be speculated on from these observations. It is possible that the stabilization of the Beaufort Gyre documented in recent studies led to increased mixed layer salinities via a reduced Ekman convergence of freshwater (Dewey et al., 2018; Meneghello et al., 2018; Zhang et al., 2016; Zhong et al., 2018), which made it easier for the "background" level of mechanical mixing to deepen the mixed layer base. Alternatively, the increased mixed layer salinity could have resulted from a net export of freshwater out of the Beaufort Gyre, implying that the Arctic Ocean could increase freshwater export to the North Atlantic should these conditions continue. Additional processes such as changing freshwater runoff and/or ice growth in winter may be contributing along with changes in Beaufort Gyre circulation (driven by changes in atmospheric circulation). This claim is supported by the increase in depth of the uppermost density surfaces (by 1.5 to 5 m) over the two time periods (implying Ekman convergence and downward Ekman pumping) alongside reduced mixed layer salinity (implying Ekman convergence of saltier waters). Regardless of the exact mechanism behind the increase in mixed layer salinity, the increased salinity is the most likely cause for the deeper mixed layers.

The simultaneous increase in mixed layer depth along with the downward displacement of density surfaces over 2006–2017 differed from previous years. In the decades prior to 2008 during the spin-up of the Beaufort Gyre, the mixed layer shoaled (Peralta-Ferriz & Woodgate, 2015), while isopycnal depths increased (Timmermans et al., 2014; Zhang et al., 2016), compared with mixed layer deepening and isopycnal deepening over 2013–2017. The deepening of isopycnal surfaces even very near the base of the mixed layer is not a direct cause of the deeper mixed layer during 2013–2017. Indirectly, if the stratification maxima had shoaled somewhat during 2006–2017, changes in mixed layer depth would likely have been less dramatic, and so isopycnal deepening aids mixed layer deepening.

5.3. Timing and Interannual Variability

There is some uncertainty in the exact timing of the increase in mixed layer depth. The shallowest mixed layers in the analysis period occurred in 2008–2009, and the trend toward greater winter mixed layer

depths may have begun during these years (Figure 3a). This would be consistent with the stabilization of the Beaufort Gyre circulation that began in 2008–2009 (Dewey et al., 2018; Krishfield et al., 2014; Meneghello et al., 2018; Timmermans et al., 2014; Zhang et al., 2016). We have chosen to present the change in mixed layer depth as between time periods of 2006–2012 versus 2013–2017 as this corresponds to the observed change in mixed layer density (Figure 3b); it approximately divides the ITP record in half and corresponds to well separated statistics of mixed layer depth (Figure 3c).

The increase in mixed layer depth occurred over a period of less than 5 years and suggests that the sparse winter observations available during the past 30 years may have undersampled significant interannual variability. As a result, estimated trends of persistent decadal shoaling may be biased. Both existing and future numerical modeling studies should be used to investigate changes in mixed layer depth on interannual to decadal timescales. However, realistic numerical modeling may be hindered due to the lack of spatially and temporally varying fields (of river runoff for example) with which to force models in past decades.

5.4. Cautions and Implications

A full picture of how the mixed layer has changed is only obtained by considering several measures of salinity, density, and freshwater. As noted previously, density at the base of the mixed layer differs from the average density of the mixed layer; the former is a better measure of entrainment potential, and the latter is indicative of changes to average density (or salinity) conditions. There is also an important distinction between mixed layer salinity, which increased, and freshwater content, which decreased, between the two time periods. Liquid freshwater content relative to $S = 34.8$ g/kg (section 3, ~400-m depth) was 20.6 m over 2006–2012 and 21.3 m over 2013–2017, an increase of 0.7 m. Even when considering the region above the 29.2 g/kg salinity surface (or approximately the 1,023.5 kg/m^3 isopycnal that consists of the mixed layer and a few meters of water beneath it), freshwater content increased (slightly) from 7.4 m over 2006–2012 to 7.5 m over 2013–2017. These uppermost tens of meters consist of waters that are saltier in comparison to previous years but fresher compared to waters below, so it is the deepening of the (relatively fresh) mixed layer that results in increased freshwater content.

While we have focused on salinity and density, one consequence of a deepening mixed layer is the potential erosion of any wintertime near-surface temperature maximum layer. There was no evidence of a winter time near-surface temperature maximum (Jackson et al., 2010; Maykut & McPhee, 1995; Steele et al., 2011) within the mixed layer in the averaged winter time temperature profiles for either time period (Figure 4a). Note that mixed layer temperature was 0.03 °C cooler on average over 2013–2017 (Figure 4a), due to the increase in mixed layer salinity that reduced the freezing temperature of sea water. This is again in contrast to past observations of warming and freshening of the winter mixed layer (Jackson et al., 2011).

Regardless of the exact cause of changes in mixed layer depth, there are implications for the present and future Arctic system. It is inconclusive, from this analysis alone, whether or to what extent freshwater is being exported from the Beaufort Gyre, as an increase in mixed layer salinity can also result from decreased ice melt, increased ice growth, or decreased river runoff. The reduced stratification and increased heat content over 2013–2017 suggests a future western Arctic where one-dimensional vertical mixing increasingly brings heat into the mixed layer. Even though past observations (Maykut & McPhee, 1995; Shaw et al., 2009; Toole et al., 2010) and the present study conclude that it is difficult to vertically mix Pacific Summer Water heat into the mixed layer to melt ice, this conclusion should continue to be re-evaluated in the future, especially if mixed layer salinity increases further. Taking a three-dimensional view (as in Timmermans et al., 2014), the increased mixed layer density likely affects the proportion of Pacific Summer Water that subducts more or less adiabatically beneath the mixed layer versus being incorporated within the mixed layer to impact the ice cover or warm the atmosphere. Had the mixed layer continued to freshen and shoal, the Pacific Summer Water layer would likely have contained even more heat than it does at present. The future evolution of the mixed layer and stratification at the base of the mixed layer will continue to influence and be influenced by, the evolution of the ice cover and upper ocean water masses.

6. Summary and Conclusions

The changes observed over 2006–2017 are in contrast to those over 1980–2008. The observed mixed layer reported here was 9-m deeper and ~1 g/kg saltier over 2013–2017 compared with 2006–2012. The increase

in mixed layer salinity, and so in density, consequently weakened the stratification at the base of the mixed layer as well. This is a distinct change from the 0.64 m/year shoaling trend and 0.19 psu/year freshening trend reported by Peralta-Ferriz and Woodgate (2015).

The changes to mixed layer depth were associated with increased mixed layer salinity that cannot be explained by one-dimensional vertical mixing. We therefore infer that changes to freshwater storage and accumulation and/or release occurred between 2006 and 2017. These observations are insufficient to determine the cause of this salinity increase. However, it may have resulted from a decrease in the convergence of fresh surface waters ultimately driven by changes to atmospheric circulation (e.g., Proshutinsky et al., 2009), or a convergence of saltier waters resulting from changes to river runoff or ice growth/melt. Continued downward Ekman pumping of the upper density surfaces did not oppose the increase in mixed layer depth and potentially made it easier for existing mechanical mixing to deepen the mixed layer base as the freshwater eroded. Our understanding of the Arctic system would be improved by monitoring several aspects of the ocean in addition to freshwater storage, including ocean turbulence and vertical mixing.

Acknowledgments
We gratefully acknowledge J. Toole for helpful conversations. S. Cole was supported by the National Science Foundation under grant PLR-1602926 and J. Stadler by the Woods Hole Oceanographic Institution Summer Student Fellowship program. Profile data are available via the Ice-Tethered Profiler program website: http://whoi.edu/itp. SSM/I ice concentration data were downloaded from the National Snow and Ice Data Center.

References

Aagaard, E., & Carmack, E. C. (1989). The role of sea ice and other fresh water in the Arctic circulation. *Journal of Geophysical Research*, *94*(C10), 14,485–14,489. https://doi.org/10.1029/JC094iC10p14485

Armitage, T. W. K., Bacon, S., Ridout, A. L., Petty, A. A., Wolbach, S., & Tsamados, M. (2017). Arctic Ocean surface geostrophic circulation 2003-2014. *The Cryosphere*, *11*(4), 1767–1780. https://doi.org/10.5194/tc-11-1767-2017

Carmack, E., Polyakov, I., Padman, L., Fer, I., Hunke, E., Hutchings, J., et al. (2015). Toward quantifying the increasing role of oceanic heat in sea ice loss in the new Arctic. *Bulletin of the American Meteorological Society*, *96*(12), 2079–2105. https://doi.org/10.1175/BAMS-D-13-00177.1

Cavalieri, D. J., Parkinson, C. L., Gloersen, P., & Zwally, H. (1996, updated 2017). Sea ice concentrations from Nimbus-7 SSMR and DMSP SSM/I-SSMIS passive microwave data, version 1. Boulder, CO: NASA National Snow and Ice Data Center Distributed Active Archive Center. https://doi.org/10.5067/8GQ8LZQVL0VL

Comiso, J. C. (2012). Large decadal decline in the Arctic multiyear ice cover. *Journal of Climate*, *25*(4), 1176–1193. https://doi.org/10.1175/JCLI-D-11-00113.1

D'Asaro, E. A., & Morison, J. H. (1992). Internal waves and mixing in the Arctic Ocean. *Deep Sea Research*, *39*(2), S459–S484. https://doi.org/10.1016/S0198-0149(06)80016-6

Dewey, S., Morison, J., Kwok, R., Dickinson, S., Morison, D., & Andersen, R. (2018). Arctic ice-ocean coupling and gyre equilibration observed with remote sensing. *Geophysical Research Letters*, *45*(3), 1499–1508. https://doi.org/10.1002/2017GL076229

Guthrie, J. D., Morison, J. H., & Fer, I. (2013). Revisiting internal waves and mixing in the Arctic Ocean. *Journal of Geophysical Research: Oceans*, *118*, 3966–3977. https://doi.org/10.1002/jgrc.20294

Jackson, J. M., Allen, S. E., McLaughlin, F. A., Woodgate, R. A., & Carmack, E. C. (2011). Changes to the near-surface waters in the Canada Basin, Arctic Ocean from 1993-2009: A basin in transition. *Journal of Geophysical Research*, *116*, C10008. https://doi.org/10.1029/2011JC007069

Jackson, J. M., Carmack, E. C., McLaughlin, F. A., Allen, S. E., & Ingram, R. G. (2010). Identification, characterization, and change of the near-surface temperature maximum in the Canada Basin, 1993-2008. *Journal of Geophysical Research*, *115*, C05021. https://doi.org/10.1029/2009JC005265

Krishfield, R., Toole, J., & Timmermans, M.-L. (2008). ITP data processing procedures (Tech Rep. 24 pp.). Woods Hole Oceaongraphic Institute. Retrieved from http://www.whoi.edu/fileserver.do?id=35803&pt=2&p=41486

Krishfield, R. A., Proshutinsky, A., Tateyama, K., Williams, W. J., Carmack, E. C., McLaughlin, F. A., & Timmermans, M.-L. (2014). Deterioration of perennial sea ice in the Beaufort Gyre from 2003 to 2012 and its impact on the oceanic freshwater cycle. *Journal of Geophysical Research: Oceans*, *119*, 1271–1305. https://doi.org/10.1002/2013JC008999

Kwok, R., Cunningham, G. F., Wensnahan, M., Rigor, I., Zwally, H. J., & Yi, D. (2009). Thinning and volume loss of the Arctic Ocean sea ice cover: 2003-2008. *Journal of Geophysical Research*, *114*, C07005. https://doi.org/10.1029/2009JC005312

Kwok, R., Spreen, G., & Pang, S. (2013). Arctic sea ice circulation and drift speed: Decadal trends and ocean currents. *Journal of Geophysical Research: Oceans*, *118*, 2408–2425. https://doi.org/10.1002/jgrc.20191

Maykut, G. A., & McPhee, M. G. (1995). Solar heating of the Arctic mixed layer. *Journal of Geophysical Research*, *100*(C12), 24,691–24,703. https://doi.org/10.1029/95JC02554

McPhee, M. G. (2012). Advances in understanding ice-ocean stress during and since AIDJEX. *Cold Regions Science and Technology*, *76-77*, 24–36. https://doi.org/10.1016/j.coldregions.2011.05.001

McPhee, M. G. (2013). Intensification of geostrophic currents in the Canada Basin, Arctic Ocean. *Journal of Climate*, *26*(10), 3130–3138. https://doi.org/10.1175/JCLI-D-12-00289.1

Meneghello, G., Marshall, J., Timmermans, M.-L., & Scott, J. (2018). Observations of seasonal upwelling and downwelling in the Beaufort Sea mediated by sea ice. *Journal of Physical Oceanography*, *48*(4), 795–805. https://doi.org/10.1175/JPO-D-17-0188.1

Peralta-Ferriz, C., & Woodgate, R. A. (2015). Seasonal and interannual variability of pan-Arctic surface mixed layer properties form 1979 to 2012 from hydrographic data, and the dominance of stratification for multiyear mixed layer depth shoaling. *Progress in Oceanography*, *134*, 19–53. https://doi.org/10.1016/j.pocean.2014.12.005

Proshutinsky, A., Krishfield, R., Timmermans, M.-L., Toole, J., Carmack, E., McLaughlin, F., et al. (2009). Beaufort Gyre freshwater reservoir: State and variability from observations. *Journal of Geophysical Research*, *114*, C00A10. https://doi.org/10.1029/2008JC005104

Regan, H. C., Lique, C., & Armitage, T. W. K. (2019). The Beaufort Gyre extent, shape, and location between 2003 and 2014 from satellite observations. *Journal of Geophysical Research: Oceans*, *124*, 844–862. https://doi.org/10.1029/2018JC014379

Shaw, W. J., Stanton, T. P., McPhee, M. G., Morison, J. H., & Martinson, D. G. (2009). Role of the upper ocean in the energy budget of Arctic sea ice during SHEBA. *Journal of Geophysical Research*, *114*, C06012. https://doi.org/10.1029/2008JC004991

Steele, M., Ermold, W., & Zhang, J. (2011). Modeling the formation and fate of the near-surface temperature maximum in the Canadian Basin of the Arctic Ocean. *Journal of Geophysical Research*, *116*, C11015. https://doi.org/10.1029/2010JC006803

Timmermans, M.-L., Cole, S., & Toole, J. (2012). Horizontal density structure and restratification of the Arctic Ocean surface layer. *Journal of Physical Oceanography*, *42*(4), 659–668. https://doi.org/10.1175/JPO-D-11-0125.1

Timmermans, M.-L., Proshutinsky, A., Golubeva, E., Jackson, J. M., Krishfield, R., McCall, M., et al. (2014). Mechanisms of Pacific Summer Water variability in the Arctic's Central Canada Basin. *Journal of Geophysical Research: Oceans*, *119*, 7523–7548. https://doi.org/10.1002/2014JC010273

Timmermans, M.-L., Toole, J., & Krishfield, R. (2018). Warming of the interior Arctic Ocean linked to sea ice losses at the basin margins. *Science Advances*, *4*, eaat6773. https://doi.org/10.1126/sciadv.aat6773

Toole, J. M., Krishfield, R. A., Timmermans, M.-L., & Proshutinsky, A. (2011). The Ice-Tethered Profiler: Argo of the Arctic. *Oceanography*, *24*(3), 126–135. https://doi.org/10.5670/oceanog.2011.64

Toole, J. M., Timmermans, M.-L., Perovich, D. K., Krishfield, R. A., Proshutinsky, A., & Richter-Menge, J. A. (2010). Influences of the ocean surface mixed layer and thermohaline stratification on Arctic Sea ice in the central Canada Basin. *Journal of Geophysical Research*, *115*, C10018. https://doi.org/10.1029/2009JC005660

Zhang, J., Steele, M., Runciman, K., Dewey, S., Morison, J., Lee, C., et al. (2016). The Beaufort Gyre intensification and stabilization: A model-observation synthesis. *Journal of Geophysical Research: Oceans*, *121*, 7933–7952. https://doi.org/10.1002/2016JC012196

Zhong, W., Steele, M., Zhang, J., & Cole, S. T. (2018). Circulation of Pacific Winter Water in the western Arctic Ocean. *Journal of Geophysical Research: Oceans*, *124*, 863–881. https://doi.org/10.1029/2018JC014604